Title: Inkjet printing of transdermal microneedles for the delivery of anticancer agents

Author: Md Jasim Uddin Nicolaos Scoutaris Pavlos Klepetsanis Babur Chowdry Mark R. Prausnitz Dennis Douroumis

PII: S0378-5173(15)00062-9
DOI: http://dx.doi.org/doi:10.1016/j.ijpharm.2015.01.038
Reference: IJP 14621

To appear in: *International Journal of Pharmaceutics*

Received date: 13-10-2014
Revised date: 15-1-2015
Accepted date: 20-1-2015

Please cite this article as: Uddin, Md Jasim, Scoutaris, Nicolaos, Klepetsanis, Pavlos, Chowdry, Babur, Prausnitz, Mark R., Douroumis, Dennis, Inkjet printing of transdermal microneedles for the delivery of anticancer agents.International Journal of Pharmaceutics http://dx.doi.org/10.1016/j.ijpharm.2015.01.038

Inkjet printing of transdermal microneedles for the delivery of anticancer agents

Md Jasim Uddin[1], Nicolaos Scoutaris[1], Pavlos Klepetsanis[2], Babur Chowdry[1], Mark R. Prausnitz[3], Dennis Douroumis[1,*]D.Douroumis@gre.ac.uk

[1] School of Science, Faculty of Engineering and Science, University of Greenwich, Medway Campus, Chatham Maritime, Kent, ME4 4TB, UK

[2]Laboratory of Pharmaceutical Technology, Department of Pharmacy, University of Patras, Rio 26510, Greece

[3]School of Chemical and Biomolecular Engineering, Georgia Institute of Technology, Atlanta, GA 30332, USA

[*] Corresponding author.

Graphical abstract

ABSTRACT

A novel inkjet printing technology is introduced as a process to coat metal microneedle arrays with three anticancer agents 5-fluororacil, curcumin and cisplatin for transdermal delivery. The hydrophilic graft copolymer Soluplus® was used as a drug carrier and the coating formulations consisted of drug – polymer solutions at various ratios. A piezoelectric dispenser jetted microdroplets on the microneedle surface to develop uniform, accurate and reproducible coating layers without any material losses. Inkjet printing was found to depend on the nozzle size, the applied voltage (mV) and the duration of the pulse (μs). The drug release rates were determined *in vitro* using Franz type diffusion cells with dermatomed porcine skin. The drug release rates depended on the drug–polymer ratio, the drug

lipophilicity and the skin thickness. All drugs presented increased release profiles (750 μm skin thickness), which were retarded for 900 μm skin thickness. Soluplus assisted the drug release especially for the water insoluble curcumin and cisplatin due to its solubilizing capacity. Inkjet printing was proved an effective technology for coating of metal microneedles which can then be used for further transdermal drug delivery applications.

Keywords: inkjet printing, microneedles, release, transdermal delivery, anticancer drugs.

INTRODUCTION

Microneedles (MNs) are attractive medical devices for transdermal delivery for a wide range of active substances such as vaccines, proteins, anticancer drugs, oligonucleotides and DNA (Arora et al., 2008; Chabri et al., 2004; Katikaneni et al., 2009; Kim et al., 2014; Li et al., 2009; Lin et al., 2001). MNs facilitate the passing of therapeutic agents through the stratum corneum by creating micro-channels (Chen et al., 2012; Choi et al., 2012; Lee et al., 2008) by piercing the skin. Thus, MNs can increase the *in vitro* permeability of the drugs by orders of magnitude such as small molecules and proteins (Henry et al., 1998; McAllister et al., 2003). Previous studies have also demonstrated that MNs are capable of piercing skin in a painless manner making them suitable for patients who suffer from needlephobia when using hypodermic needles (Nir et al., 2003; Simonsen et al., 1999). In addition, human and animal studies have shown that intradermal immunization is more dose effective compared to intramascular or subcutaneous administration (Chen et al., 2011; van der Maaden et al., 2012).

There are four different approaches of microneedle – based drug delivery. Such approaches involve a) piercing of solid MNs into the skin and subsequent application of a drug patch on the targeted site, b) coating of a drug onto the MN surface and piercing into the skin followed by drug dissolution within the skin, c) manufacturing of biodegradable of polymeric MNs with encapsulated drug for controlled release after piercing and d) using hollow MNs allowing injection of a drug solution. The first approach is limited due to the fact that microchannels do not remain open for long time periods preventing effective delivery of the actives. Hollow MNs require a stable solution while the administration is not straightforward (i.e. blocking of MN holes, not easy for self-administration). Polymeric MNs

composed of water-soluble polymers are difficult to insert fully in the skin due to their geometries and inferior mechanical strength (Kochhar et al., 2013; Larrañeta et al., 2014; Lee et al., 2011). As a result they present incomplete insertion leading to ineffective drug delivery and material waste.

From these approaches coated metal MNs are an attractive alternative for fast acting delivery due to their superior insertion ability and improved delivery efficiency. Metal MNs are cost effective, can be self-administrated and deliver a wide range of therapeutic substances. In addition, the application of coating layers on the MN surface promotes their long-term stability, as the active substances are present in a solid state. Despite the several advantages of metal microneedles the coating process remains problematic due to the limited dose control, content uniformity, material wastes and small range of coated actives. In the past several coating technologies have been proposed such as dip-coating, roll coating and spray coating without however being very successful (Bierwagen, 1992). Currently dip-coating is the preferred technology, which involves dipping the MN arrays in a polymeric solution several times until a uniform film is created on the needle surface. Nevertheless, dip – coating of solid MNs requires the optimization of coating solutions with suitable viscosities and has a few important drawbacks. These include uncontrollable material deposition on the substrate, bulky layers around the metal surface, weight variations of coated arrays, limited drug loading, material waste and limited scale -up.

In order to overcome these drawbacks it is essential to introduce innovative coating approaches. Inkjet printing is a novel approach that can be employed for the coating of transdermal MNs by dispensing a wide range of active substances in the form of tiny droplets that form uniform layers on the needle surface. A piezoelectric microdispenser generates droplets in a drop – on – demand manner when the ceramic actuator is triggered. The droplet size is controlled by adjusting the piezo parameters such as amplitude, pulse width and excitation frequency. Inkjet printing has been used for coating of miniaturized devices such as stents by applying thin coatings of active polymer formulations (Tarcha et al., 2007). In the current study inkjet printing was employed to coat metal microneedles with anticancer drug formulations by applying uniform, accurate and reproducible coatings. The effect of drug lipophilicity, drug loading and formulation composition on the drug release profiles was evaluated.

2. Materials and methods

2.1 Materials

Soluplus-® a co-polymer of polyvinyl caprolactame-polyvinyl acetate-polyethylene was donated by BASF (Ludwigshafen, Germany). Curcumin (CRC, >94%), 5-fluorouracil (5-FU, >99%), *cis*-platin (CPT, >99%)) and sodium fluorescein (FlNa) were purchased from Sigma-Aldrich, UK. Padgett Dermatome and dermatome blades were purchased from Integra Life™ Sciences Corporation (PA, USA), KH2PO4, $Na_2HPO_4.12H_2O$, NaCl, KCl, NaOH, HCl, acetonitrile, acetic acid, methanol, ethanol, phosphoric acid and hydrochloric acid were purchased from Fisher Scientific (Loughborough, UK).

2.2 Microneedle Fabrication

Arrays of solid microneedles were fabricated by cutting needle structures from stainless steel sheets (SS 304, 75μm thick; McMaster-Carr, Atlanta, GA, USA) using an infrared laser (Resonetics Maestro, Nashua, NH, USA). Initially, the shape and orientation of the arrays were drafted in a CAD file (AutoCAD; Autodesk, Cupertino, CA, USA), by using the laser-control software. The laser beam traced the desired shape of the needle, which ablated the metal sheet and created the needles in the plane of the sheet. The laser was operated at 1000 Hz at an energy density of 20 J/cm2 and required approximately 4 min to cut an array. The metal sheet with needles on it was cleaned in hot water (Alconox, White Plains, NY, USA) and rinsed with DI water. Each needle was then manually bent at 90° out of the plane of the sheet. The needles were electropolished in a bath containing a 6:3:1 mixture by volume of glycerin, phosphoric acid, and water (Fisher Scientific, Atlanta, GA, USA) to remove debris (Graham 1971; Hensel, 2000). This electropolishing process reduced the needle thickness to 50 μm.

2.3 Coating formulations

Polymers were dissolved in deionized water or ethanol (EtOH) prior to the addition of drug molecules. The resulting formulations were left for 24hr at 50 rpm in a shaker (Brunswick Scientific, USA) to achieve complete dissolution. Three model anticancer drugs, 5-FU, CRC and CPT, were used to develop uniform and reproducible coating layers on the metallic MN arrays. FlNa was used as a control model substance due to its high water solubility. The compositions of the jetted formulations are shown in Table 1.

2.4 Inkjet printing process for MN coating

Inkjet printing was conducted with a Nanoploter II (Gesim, Germany) where the MNs are mounted on a specifically designed holder and positioned at 45º relative to the dispenser (Fig. 1). The drug/polymer solutions were jetted through a piezodriven dispenser (PicPip 300) onto the MN surface in the form of fine droplets of 300 pl approximately. The appropriate drug/polymer amounts were coated through various coating cycles. For each coating cycle, 4 dots of a coating formulation were dispensed longitudinally to the axis of each MN and the process was repeated for 1, 2 or 5 jetting cycles to coat the desired amounts. The dispenser is a piezoelectric ceramic that is deformed upon voltage appliance, thus ejecting a droplet from the nozzle at a speed 1-5m/s ("drop on demand"). Due to the MN design a simple coating algorithm that targets the needle edge was designed. The operation process is controlled by an oscilloscope, which controls if the dispenser jets according to the desired standard droplet size. Stroboscopic image capture provides real-time analysis of pipette performance both before and after sample dispensing. The droplet diameter allows estimation of the dispensed volume calculated through image analysis. If, for any reason, a sample is not dispensed as instructed (e.g. empty sample well), the software logs this and allows for repetition of respective sample printing, thus ensuring completion of the task.

2.5 Skin preparation for *in-vitro* MN testing

Abdominal pigskin was obtained from a local slaughterhouse (Forge Farm Ltd, Kent) and excised to the required thickness using an electrically driven dermatome (Integra Life Sciences™, Padgett Instruments, NJ, USA). The dermatomed skin was then preserved at 4ºC until required. Skin samples were left for 15 minutes at room temperature before being used for MN array experiments. The thickness of skin was measured by using a micrometer after placing a cover slip as a support base. The thickness of the cover slip was measured alone followed by the skin and cover slip together; the actual thickness was determined by subtracting one measurement from the other. Tissue disks of the required dimensions were cut for the Franz diffusion cells using a blade. The skin tissue (750-900 μm thick) was placed in PBS (pH 7.4) for 2 hr.

2.6 I*n-vitro* permeability studies by using Franz diffusion cells

The skin samples were mounted on the donor compartment of Franz diffusion cells (Permegear Inc.). A fraction collector (Gilson FC 204, Middleton, USA) was attached to the water bath (Thermofisher scientific, Newington, USA) and PBS was supplied through a

pump (Minipuls 2, Gilson, Luton, UK). Each Franz cell was calibrated precisely with PBS at a rate of 6 ml/hr. The receptor arms were sealed with a plastic cap and the donor compartments were sealed with a cover slip to avoid sample evaporation. The Franz cells were maintained at 37ºC and the skin surface temperature was maintained at 32ºC. The Franz cells were equilibrated up to 30 minutes before introducing test formulations to the donor compartments. The integrity of the epidermal skin sheets was monitored for a while prior to each experiment.

Dermatomed skin was placed in a Petri dish containing PBS (pH 7.4) buffer solution. The drug coated MN arrays were applied for 30s onto the skin with an applied force of 7N using the TA HD *plus* texture analyser (Stable micro system, Surrey, UK). Dislodgement of the MN arrays was prevented using an adhesive tape (3M, UK). Subsequently, the skin samples with the inserted MN arrays were mounted in the Franz diffusion cells with the stratum corneum on the topside. The drug cumulative release was measured for each formulation in triplicates.

2.7 HPLC analysis

The 5-FU and CRC samples were determined by using HPLC analysis. An Agilent Technologies 1200 series HPLC system (Agilent Technologies, Cheshire, UK) comprising an autosampler, a quaternary HPLC pump and a photodiode array detector, a Sunfire TM – C18 column (250 x 4.6 mm, particle size 5 µm; Waters, Ireland) range was used. For the 5-FU the mobile phase comprised of water/ethanol and H_3PO_4 at a ratio of 65:30:0.5 (V/V/V) at a flow rate of 1 ml/ml was used. UV absorbance was measured at 266 nm using a photodiode-array, the column temperature was set at 30°C and the injection volume was 50 µl. For the CRC analysis a 10 cm HICHROM Valco column (CHROM Ltd) and the mobile phase consisted of acetonitrile/methanol/water/acetic acid at a ratio of 49:20:30:1. The flow rate was 1.5 ml/min, injection volume was 20 µL and the absorbance was recorded at 425 nm. The recordings were integrated using the Chemstation® software.

The drug amounts coated on the MN arrays were quantified by placing the MN arrays in 50 ml of deionised water. Sonication, for 15-20 mins, was used to dissolve the coating layers and the free drug was determined by HPLC analysis.

2.8 Atomic absorption spectroscopic analysis of CPT

The total platinum in CPT was determined using graphite furnace atomic absorption spectroscopy (GFAAS). A computer controlled atomic absorption spectrometer (Analyst 300,

Perkin Elmer) equipped with a graphite furnace (HGA-800, Perkin Elmer) was used. The absorption was measured at a wavelength of 0.70nm or 265.9nm slit bandwidth. A deuterium lamp was used for continuous background correction to eliminate spectral interferences. Pyrolytic graphite coated tubes without integrated platform were used and the atomization process was performed on the tube wall. High purity argon (99.99+ %) at a flow rate of 250 ml/min was used as a purge gas and its flow was interrupted during the atomization step. An aqueous platinum standard solution of 1000 mg/ml Pt (Chem-Lab NV) and an intermediate solution of 5 mg/l Pt (using 0.2% nitric acid as diluent) were prepared. Calibration standards (25-300 ppb) were prepared daily from the intermediate solution, using 0.2 % nitric acid as diluent and stored in polyethylene containers. The linear range was found to be between 0 and 300 ppb (μg/l). The reagent blanks and calibration standards were measured in triplicate, whilst the platinum sample was evaluated in quadruplicate. A 10μl aliquot of standard/sample was transferred on to the wall of the pyrolytic graphite coated tube using a high precision pipette. High purity water, obtained by distilling triply deionized water was used throughout this study.

3. Results and discussion

For the purposes of the study 2D solid metal MNs fabricated by laser cutting and electropolishing were used. Each MN array consisted of single rows of five microneedles (50 in total) with 700 μm length, 200μm width from the base and 50μm thickness. Previous studies (Kim et al., 2010) have shown that coating of MNs requires proper design of coating formulations in order to achieve uniform coatings and avoid the creation of bulky layers. As shown in Table 2 the coating solutions composed of three anticancer agents, 5FU, CRC and CPT, with different water solubilities and the graft water soluble polymer Soluplus. The polymer was selected due to its capacity to increase solubility of water insoluble and hence dissolution rates and it has not previously used in MN coating applications. CRC is extremely water insoluble drug (1.1μg/100ml) while CPT has moderate water solubility (250mg/100ml) and Soluplus was expected to increase their *in vitro* release rates after coating on the needles surface. Thus coating formulations with various polymer concentrations were optimized for the delivery of the anticancer drugs.

In contrast to dip coating approaches inkjet printing requires low viscosity solutions in order to generate droplets of small particle size and to avoid blockage of the jetting nozzle (50μm). The viscosity of the coating solutions was evaluated and for all drug formulations showed

low values varying from 36–67cP. The low viscosity solutions minimized clogging of the nozzle and provided continuous MN coating without any interactions. However, continuous jetting can cause gradual polymer accumulation at the edge of the nozzle, therefore, the Nanoplotter coating patterns included a washing step with either water or ethanol. The jetting efficiency depends significantly on the nozzle size, the applied voltage (mV) on the piezoelectric materials and the pulse duration (μs). The coating optimization showed that nozzles with jetting volumes of 100pl produce small droplets but cause clogging while volumes of 300pl create slightly larger droplets (80-120μm), which can provide excellent coating on MNs with narrow width. Previous studies have shown that the ejected fluid volume and consequently the droplet size is a linear functions of the applied voltage (μs) and for a given coating solution increases droplet diameter. For the given viscosity range of the coating solutions the jetting was optimized at 100mV and 60μs, which generated droplets of 100–110 μm. The droplets had a consistent particle size without any satellites as observed from the stroboscope (Fig. 1a).

Another critical coating parameter, which plays a key role on the quality of the coating is the distance of the nozzle from the MN surface. For the miniaturized MN arrays the nozzle should be as close as possible to the needle edge to target the surface and to minimize possible material losses. For this reason the nozzle tip was positioned at a 45^{o} angle between the axis of the nozzle and the plane of the MN array. As shown in Fig. 1b the MN array is placed on an especially designed holder with the tip of the nozzle targeting just below of the needle edge. In Fig. 1c it can be clearly seen that the Nanoplotter can apply simultaneously coatings on eight MN arrays with high precision and reproducibility. This is evident in Fig. 2a, which shows a UV scan of a FlNa–POL formulation coated the MN array (3 droplets per needle). The coated FlNa is spotted only on the microneedle surface without any coatings on the substrate of the array. This observation is also supported by the SEM image in Fig. 2b, which shows high precision and reproducible coatings across the MN array. In addition, Fig. 2c shows the distribution of the fluorescent FlNa across the surface of fully coated needles. FlNa is homogeneously distributed on the needles without any substance accumulation or void areas. By rotating the MN array it was possible to coat both sides of each needle and deposit equal amounts of coating material.

Further evaluation of the coated formulations included coatings with higher drug–polymer amounts varying from 100–150μg and maximum coating drug/polymer amounts of 600 μg. Fig. 3 shows SEM images of typical 5-FU/SOL coatings jetted on the MN surface where the

needles are completely covered. The coatings appear uniform, accurate and reproducible with smooth surfaces. In addition, inkjet printing facilitated the coating of thin layers without the creation of bulky coatings even for high deposited amounts. There is no coated material on the array substrate indicating that all of the printed formulations are deposited on the needle surface without any losses. The great advantage of the developed inkjet printing approach is the targeting of the needle surface with high accuracy at different areas of the surface and droplet printing by moving along the needle length though small step increments (50μm).

The antiproliferative action of the 5-FU, CRC and CPT using MN arrays was assessed by MTT assay on A-431 human skin epidermoid carcinoma cells. As shown in Fig. 4 for all drugs the antiproliferative activity increased dose dependently. At the lowest dose (15μg/ml) no significant difference was observed and cell viability varied from 65–78%. However, as the concentration increased the drugs presented significant differences in cell viability depending on their potency. CRC was highly potent with only 7% viability (Mulik et al., 2010) at 7μg/ml followed by CPT with 9.4% at 200μg/ml. As it can be seen 5-FU was the less potent active substance with only 20% cell viability at 400μg/ml. Based on their antiproliferative activity it was decided to coat different amounts on the metal MNs for each drug (shown in Table 2).

To study the release profile of the three anticancer drugs and the control FlNa at different SOL ratios, drug loaded MNs were inserted into porcine skin and the release monitored in Franz diffusion cells for 3hrs. These drugs were selected in order to investigate the effect of drug lipophilicity, loading and the coating formulation. Two sets of experiments were conducted and MNs pierced porcine skin with thickness of 750μm and 900μm respectively. Fig. 5a shows the release of the control FlNa where the increase of SOL ratio resulted in slower release rates. For 1:1 and 1:2 FlNa/SOL ratios the release rates were rapid with 65% and 45% been released after 1hr while at 1:3 ratio controlled release was observed. After 3hr the first two formulations (C1, C2) showed complete release of FlNa. Similar results were observed for 5-FU the dissolution of SOL was the rate-limiting factor for the drug release (Fig. 5b). The 5-FU release patterns are similar to those of FlNa but with slightly lower rates most probably because of the higher water solubility of the latter. However, the 5-FU release rates were significantly slower when MNs pierced the skin with a thickness of 900μm. Fig. 5c shows that no more than 35% of FU was detected in the receptor compartment after 1hr. The lower cumulative release of both FlNa and 5-FU shows deeper skin penetration. These results are in agreement with similar studies (Donnelly et al., 2010), which showed different

permeation profiles for theophylline loaded polymeric MNs of different heights (350μm and 900μm) by piercing neonatal porcine skin or with silicon MNs with different needle lengths (ranging from 100 to 1100μm) (Yan et al., 2010). Depending on the skin thickness the drug has to diffuse different distances before finally reaching the acceptor compartment.

Fig. 6a,b show the release rates of CRC at three different drug/polymer ratios and porcine skin thickness. Interestingly the results showed rapid release rates for all CRC/SOL formulations with 56 – 96% release within 1hr. SOL was used a drug carrier due to its amphiphilic nature and proven capacity to increase the solubility and bioavailability of water insoluble drugs by acting as solubilizer (Maniruzzaman et al., 2013; Tian et al., 2014). In our case SOL demonstrated increased solubilisation capacity especially for the CRC/SOL (1:2) ratio where 96% of the drug is release after 1hr. It appears that this was the optimum CRC/SOL ratio as F4 (1:1) formulations showed also increased release rates (80%) within the first hour but it is obvious that additional polymer amounts were required to increase the release rates. Further increase in SOL content did not demonstrate further improvement and the observed CRC release was slower. From the comparison of Fig. 5a,c and Fig. 6a,b the release rates of the water insoluble CRC are faster to those of the water soluble 5-FU. However, a careful consideration of the data in Table 2 shows that the drug/polymer coated amounts of CRC are considerably lower compared to 5-FU and thus the layer of the polymeric carrier requires longer times to dissolve. When porcine skin of 900μm thickenss was used the CRC release rates were slower (Fig. 6b) and 70-80% was released for F4–F5 while only 50% of F6 was detected in the receptor compartment. Further analysis of the samples (Table 2) showed that most of the drug remained in the skin tissue after 3hr and it was completely dissolved from the needle surface.

Finally, as shown in Fig. 7a CPT presented also rapid dissolution rates for 1:1 and 1:2 drug/polymer ratios, which were almost identical. For those formulations the release rates varied from 77 – 82% after 1hr while the increase of SOL ratio resulted in slower rates (57%). Similarly to the previous drug substances for thicker skin samples the CPT release rates was retarded. Fig. 8 shows the application of methylene blue coated metal MNs on porcine skin and the creation of perforations immediately after the MN piercing (Chu and Prausnitz, 2011; Donnelly et al., 2008; Gill and Prausnitz, 2007). The staining disappears after six hours without any marks on the skin indicating successful delivery of the coating material as methylene blue diffuses in the tissue. The use of inkjet printing technology for the

active coating of MNs and their in vitro release studies drugs provided useful information for future *in vivo* animal studies.

4. Conclusions

In conclusion, inkjet printing was successfully used to apply polymeric coating of three anticancer substances on the surface of transdermal MNs. The optimization of the ink jetting processing delivered highly uniform, reproducible and accurate coating at various drug-polymer ratios. The hydrophilic 5-FU showed rapid release profiles with most of the substance been released within 3hr. Rapid release rates were also obtained for the water insoluble CRC and CPT with most of the drug amounts been released after 1hr. This was achieved by using SOL a polymer with high solubilizing capacity, which increased the drug release rates. Inkjet printing is a novel technology for coating of MN arrays compared to conventional approaches and can be further used for MN delivery.

References

Graham AK 1971. Electroplating Engineering Handbook. Van Nostrand Reinhold.

Arora, A., Prausnitz, M.R., Mitragotri, S., 2008. Micro-scale devices for transdermal drug delivery. International Journal of Pharmaceutics 364, 227-236.

Bierwagen, G.P., 1992. Film coating technologies and adhesion. Electrochimica Acta 37, 1471-1478.

Chabri, F., Bouris, K., Jones, T., Barrow, D., Hann, A., Allender, C., Brain, K., Birchall, J., 2004. Microfabricated silicon microneedles for nonviral cutaneous gene delivery. British Journal of Dermatology 150, 869-877.

Chen, M.-C., Ling, M.-H., Lai, K.-Y., Pramudityo, E., 2012. Chitosan Microneedle Patches for Sustained Transdermal Delivery of Macromolecules. Biomacromolecules 13, 4022-4031.

Chen, X., Fernando, G.J., Crichton, M.L., Flaim, C., Yukiko, S.R., Fairmaid, E.J., Corbett, H.J., Primiero, C.A., Ansaldo, A.B., Frazer, I.H., Brown, L.E., Kendall, M.A., 2011. Improving the reach of vaccines to low-resource regions, with a needle-free vaccine delivery device and long-term thermostabilization. Journal of controlled release : official journal of the Controlled Release Society 152, 349-355.

Choi, H.-J., Yoo, D.-G., Bondy, B.J., Quan, F.-S., Compans, R.W., Kang, S.-M., Prausnitz, M.R., 2012. Stability of influenza vaccine coated onto microneedles. Biomaterials 33, 3756-3769.

Chu, L.Y., Prausnitz, M.R., 2011. Separable arrowhead microneedles. Journal of controlled release : official journal of the Controlled Release Society 149, 242-249.

Donnelly, R.F., Garland, M.J., Morrow, D.I., Migalska, K., Singh, T.R., Majithiya, R., Woolfson, A.D., 2010. Optical coherence tomography is a valuable tool in the study of the effects of microneedle geometry on skin penetration characteristics and in-skin dissolution. Journal of controlled release : official journal of the Controlled Release Society 147, 333-341.

Donnelly, R.F., Morrow, D.I., McCarron, P.A., Woolfson, A.D., Morrissey, A., Juzenas, P., Juzeniene, A., Iani, V., McCarthy, H.O., Moan, J., 2008. Microneedle-mediated intradermal delivery of 5-aminolevulinic acid: potential for enhanced topical photodynamic therapy. Journal of controlled release : official journal of the Controlled Release Society 129, 154-162.

Gill, H.S., Prausnitz, M.R., 2007. Coated microneedles for transdermal delivery. Journal of controlled release : official journal of the Controlled Release Society 117, 227-237.

Henry, S., McAllister, D.V., Allen, M.G., Prausnitz, M.R., 1998. Microfabricated microneedles: a novel approach to transdermal drug delivery. Journal of pharmaceutical sciences 87, 922-925.

Hensel, K.B., 2000. Electropolishing. Metal Finishing 98, 440-448.

Katikaneni, S., Badkar, A., Nema, S., Banga, A.K., 2009. Molecular charge mediated transport of a 13 kD protein across microporated skin. International Journal of Pharmaceutics 378, 93-100.

Kim, N.W., Lee, M.S., Kim, K.R., Lee, J.E., Lee, K., Park, J.S., Matsumoto, Y., Jo, D.-G., Lee, H., Lee, D.S., Jeong, J.H., 2014. Polyplex-releasing microneedles for enhanced cutaneous delivery of DNA vaccine. Journal of Controlled Release 179, 11-17.

Kim, Y.C., Quan, F.S., Compans, R.W., Kang, S.M., Prausnitz, M.R., 2010. Formulation of microneedles coated with influenza virus-like particle vaccine. AAPS PharmSciTech 11, 1193-1201.

Kochhar, J.S., Quek, T.C., Soon, W.J., Choi, J., Zou, S., Kang, L., 2013. Effect of microneedle geometry and supporting substrate on microneedle array penetration into skin. Journal of pharmaceutical sciences 102, 4100-4108.

Larrañeta, E., Moore, J., Vicente-Pérez, E.M., González-Vázquez, P., Lutton, R., Woolfson, A.D., Donnelly, R.F., 2014. A proposed model membrane and test method for microneedle insertion studies. International Journal of Pharmaceutics 472, 65-73.

Lee, J.W., Choi, S.O., Felner, E.I., Prausnitz, M.R., 2011. Dissolving microneedle patch for transdermal delivery of human growth hormone. Small (Weinheim an der Bergstrasse, Germany) 7, 531-539.

Lee, J.W., Park, J.-H., Prausnitz, M.R., 2008. Dissolving microneedles for transdermal drug delivery. Biomaterials 29, 2113-2124.

Li, G., Badkar, A., Nema, S., Kolli, C.S., Banga, A.K., 2009. In vitro transdermal delivery of therapeutic antibodies using maltose microneedles. International Journal of Pharmaceutics 368, 109-115.

Lin, W., Cormier, M., Samiee, A., Griffin, A., Johnson, B., Teng, C.-L., Hardee, G., Daddona, P., 2001. Transdermal Delivery of Antisense Oligonucleotides with Microprojection Patch (macroflux®) Technology. Pharm Res 18, 1789-1793.

Maniruzzaman, M., Rana, M.M., Boateng, J.S., Mitchell, J.C., Douroumis, D., 2013. Dissolution enhancement of poorly water-soluble APIs processed by hot-melt extrusion using hydrophilic polymers. Drug development and industrial pharmacy 39, 218-227.

McAllister, D.V., Wang, P.M., Davis, S.P., Park, J.H., Canatella, P.J., Allen, M.G., Prausnitz, M.R., 2003. Microfabricated needles for transdermal delivery of macromolecules and nanoparticles: fabrication methods and transport studies. Proceedings of the National Academy of Sciences of the United States of America 100, 13755-13760.

Mulik, R.S., Monkkonen, J., Juvonen, R.O., Mahadik, K.R., Paradkar, A.R., 2010. Transferrin mediated solid lipid nanoparticles containing curcumin: enhanced in vitro anticancer activity by induction of apoptosis. Int J Pharm 398, 190-203.

Nir, Y., Paz, A., Sabo, E., Potasman, I., 2003. Fear of injections in young adults: prevalence and associations. The American journal of tropical medicine and hygiene 68, 341-344.

Simonsen, L., Kane, A., Lloyd, J., Zaffran, M., Kane, M., 1999. Unsafe injections in the developing world and transmission of bloodborne pathogens: a review. Bulletin of the World Health Organization 77, 789-800.

Tarcha, P.J., Verlee, D., Hui, H.W., Setesak, J., Antohe, B., Radulescu, D., Wallace, D., 2007. The application of ink-jet technology for the coating and loading of drug-eluting stents. Annals of biomedical engineering 35, 1791-1799.

Tian, B., Zhang, L., Pan, Z., Gou, J., Zhang, Y., Tang, X., 2014. A comparison of the effect of temperature and moisture on the solid dispersions: Aging and crystallization. International Journal of Pharmaceutics 475, 385-392.

van der Maaden, K., Jiskoot, W., Bouwstra, J., 2012. Microneedle technologies for (trans)dermal drug and vaccine delivery. Journal of controlled release : official journal of the Controlled Release Society 161, 645-655.

Yan, G., Warner, K.S., Zhang, J., Sharma, S., Gale, B.K., 2010. Evaluation needle length and density of microneedle arrays in the pretreatment of skin for transdermal drug delivery. Int J Pharm 391, 7-12.

Figure captions:

Fig. 1 (a) Stroboscope image capture for measuring the droplet(s) diameter. (b) A piezoelectric nozzle printing coating formulation on the microneedle array. (c) Inkjet printing configuration for coating microneedles. The array is placed on a holder at an angle of 45°.

Fig. 2 (a) UV scan image of a coated MN array with FlNa. (b) MN arrays coated via ink jet printing with high precision and accuracy. (c) Fluorescent images of coated MNs with excellent FlNa uniformity.

Fig. 3 (a and b) SEM images of coated MNs with 5-FU/SOL formulation (600 μg coating, b) 5-FU/SOL with 300 μg coating formulation.

Fig. 4 *In vitro* antiproliferative activity of the three anticancer drugs on A-431 human skin epidermoid carcinoma cells.

Fig. 5 (a) *In vitro* release profiles of FlNa/SOL (C1–C3) coating formulations using Franz diffusion cells (n = 5, 750 μg skin thickness). (b) *In vitro* release profiles of 5-FU/SOL (F1–F3) coating formulations using Franz diffusion cells (n = 5, 750 μg skin thickness). (c) *In vitro* release profiles of 5-FU/SOL (C1–C3) coating formulations using Franz diffusion cells (n = 5, 900 μg skin thickness).

Fig. 6 (a) *In vitro* release profiles of CRC/SOL (F4–F6) coating formulations using Franz diffusion cells (n = 5, 750 μg skin thickness). (b) *In vitro* release profiles of CRC/SOL (F4–F6) coating formulations using Franz diffusion cells (n = 5, 900 μg skin thickness).

Fig. 7 (a) *In vitro* release profiles of CPT/SOL (F7–F9) coating formulations using Franz diffusion cells (n = 5, 750 μg skin thickness). (b) *In vitro* release profiles of CPT/SOL (F7–F9) coating formulations using Franz diffusion cells (n = 5, 900 μg skin thickness).

Fig. 8 Digital images of porcine skin showing successful delivery across the skin at various time intervals (0–24 h).

Table 1: Compositions of aqueous and organic solutions for 5-FU, CPT, CRC and FlNa respectively.

Formulation	Drug Substance	Drug (%)	Polymer (%)
F1	5-FU	3.0	9.0
F2	5-FU	3.0	6.0
F3	5-FU	3.0	3.0
F4	CRC	3.0	9.0
F5	CRC	3.0	6.0
F6	CRC	3.0	3.0
F7	CPT	3.0	9.0
F8	CPT	3.0	6.0
F9	CPT	3.0	3.0
C1	FlNa	3.0	9.0
C2	FlNa	3.0	6.0
C3	FlNa	3.0	3.0

Table 2: Drug/polymer coated amounts on metal MNs and solution viscosities of the coating formulations.

Form.	Drug	Drug/Polymer (μg)	Viscosity (cP)	Drug in receptor (μg)	Drug in skin (μg)
F1	5-FU	150/150	36.3±0.2	118.6±4.8	30.5±3.2
F2	5-FU	150/300	44.5±0.5	109.4±1.1	40.2±3.5
F3	5-FU	150/450	63.1±0.6	85.9±1.8	61.6±2.5
F4	CRC	50/50	-	35.5±0.8	11.1±2.5
F5	CRC	50/100	-	40.7±0.4	9.4±3.6
F6	CRC	50/150	-	24.3±0.5	20.5±4.8
F7	CPT	50/50	39.6±0.3	35.4±1.0	11.7±4.2
F8	CPT	50/100	46.7±0.4	33.2±0.8	13.8±2.8
F9	CPT	50/150	66.5±0.3	24.2±0.6	22.4±3.7
C1	FlNa	150/150	36.1±0.2	-	-
C2	FlNa	150/300	44.8±0.6	-	-
C3	FlNa	150/450	62.7±0.6	-	-

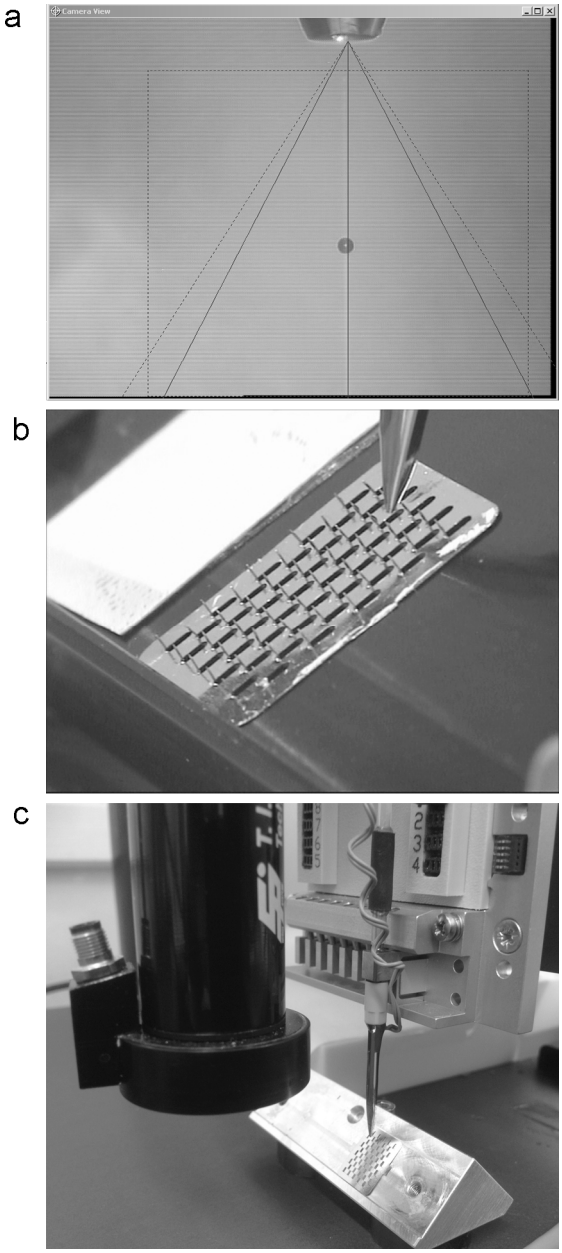

Fig. 1

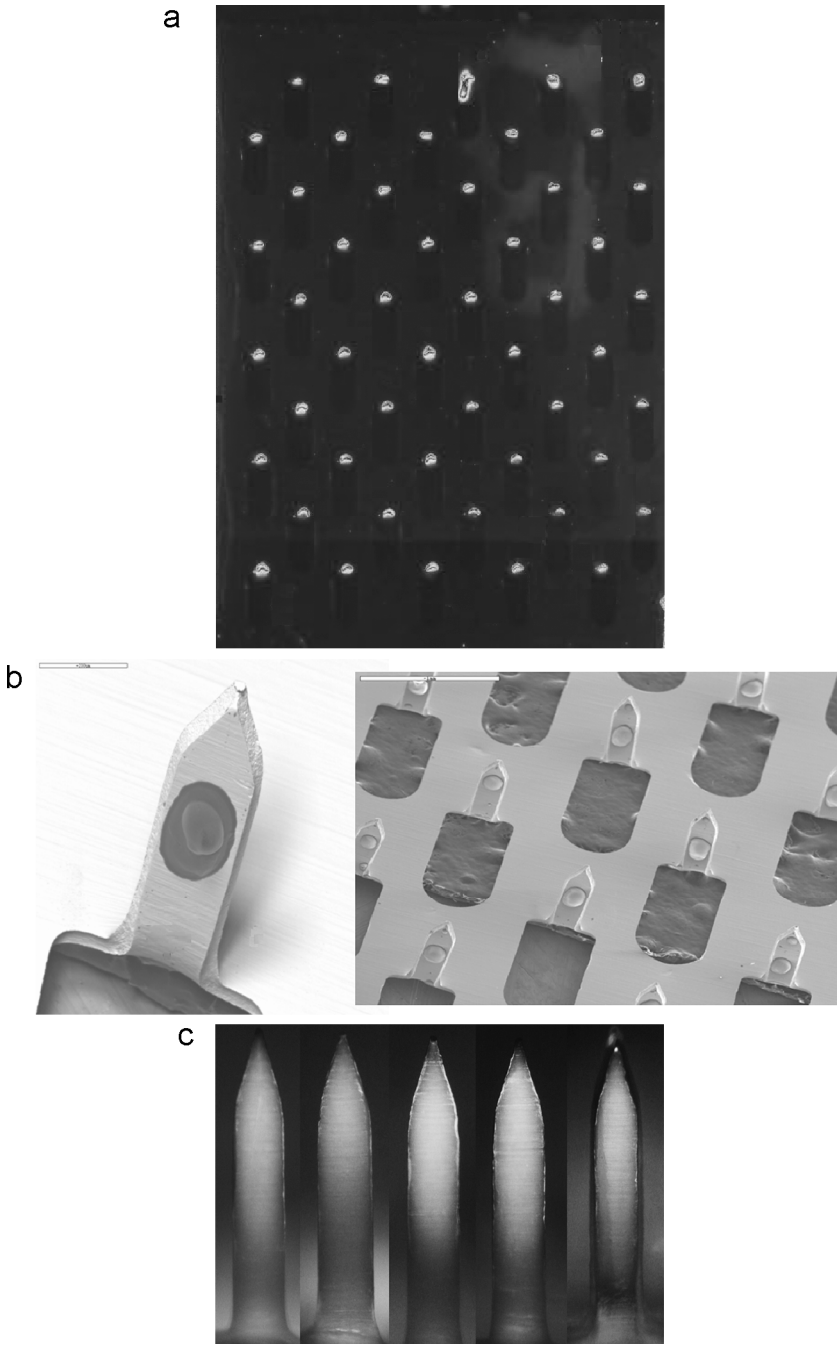

Fig. 2

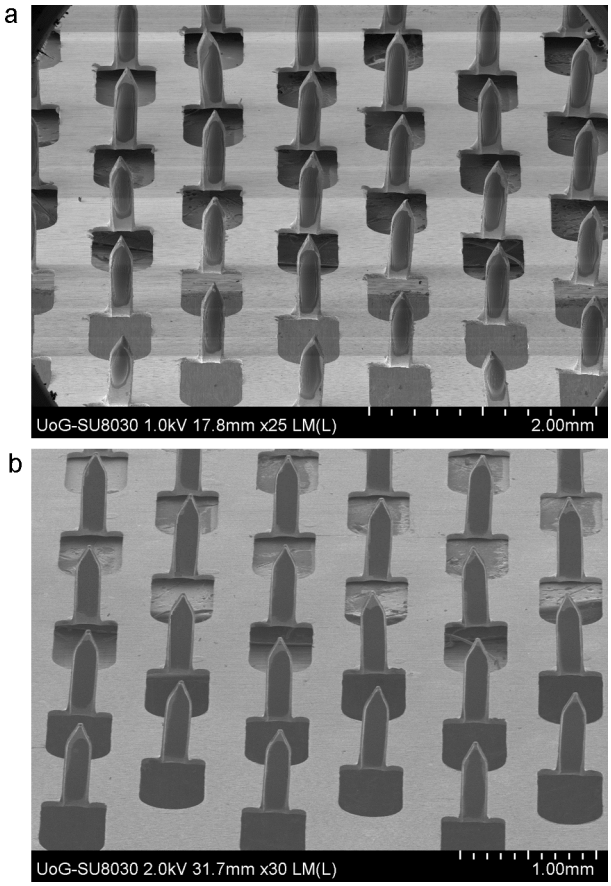

Fig. 3

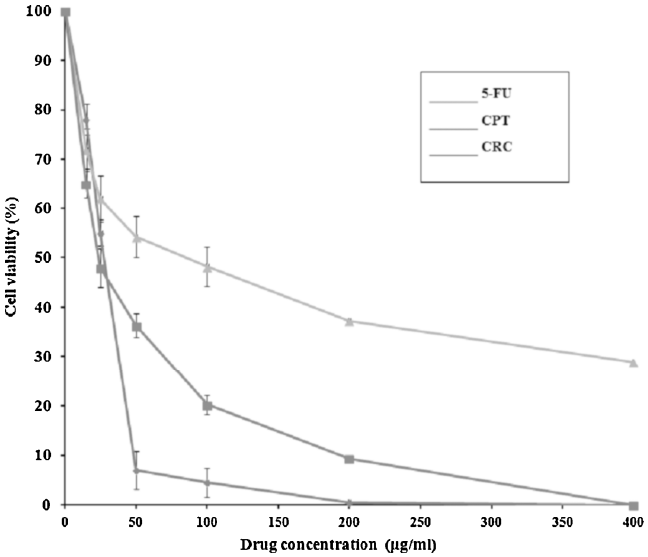

Fig. 4

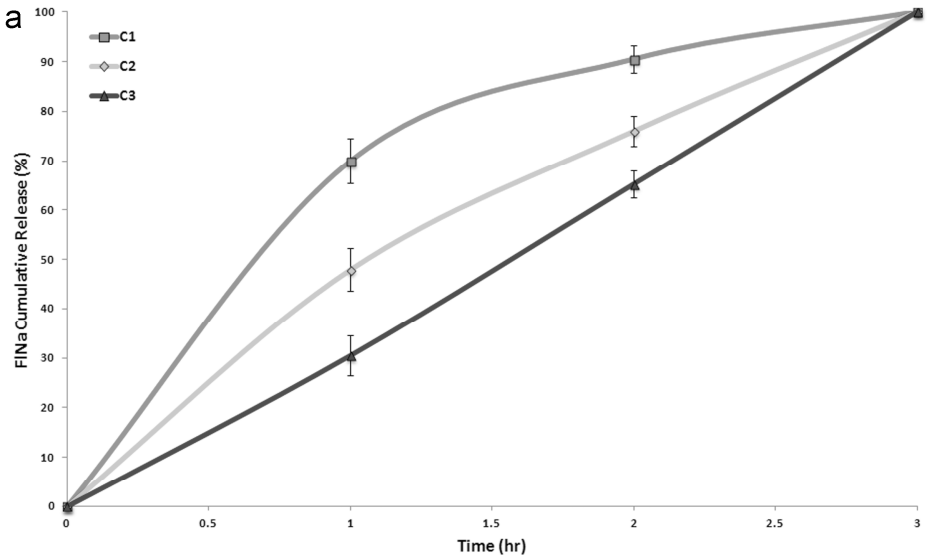

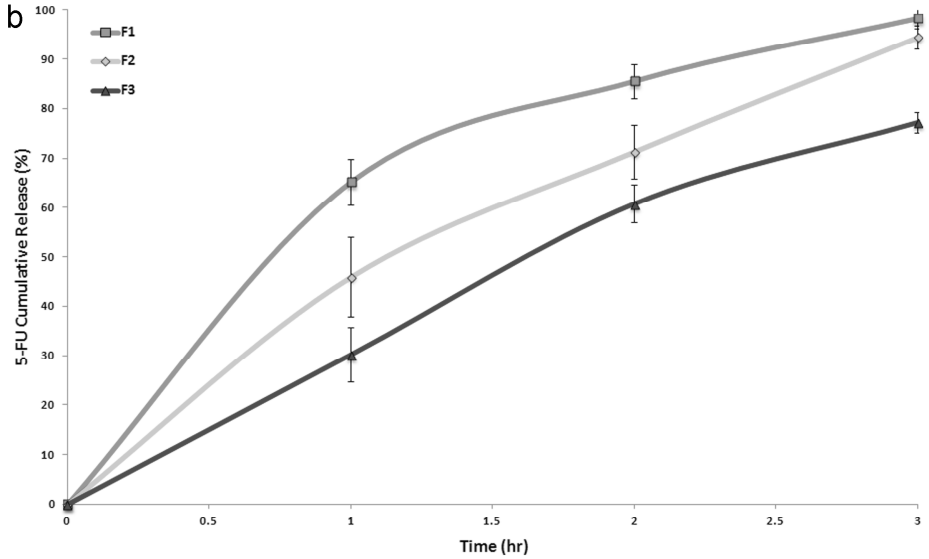

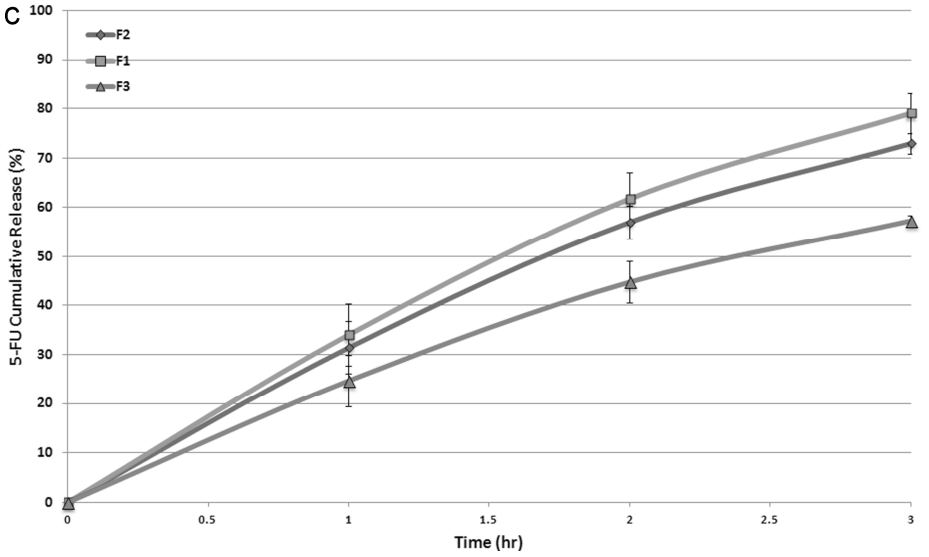

Fig. 5

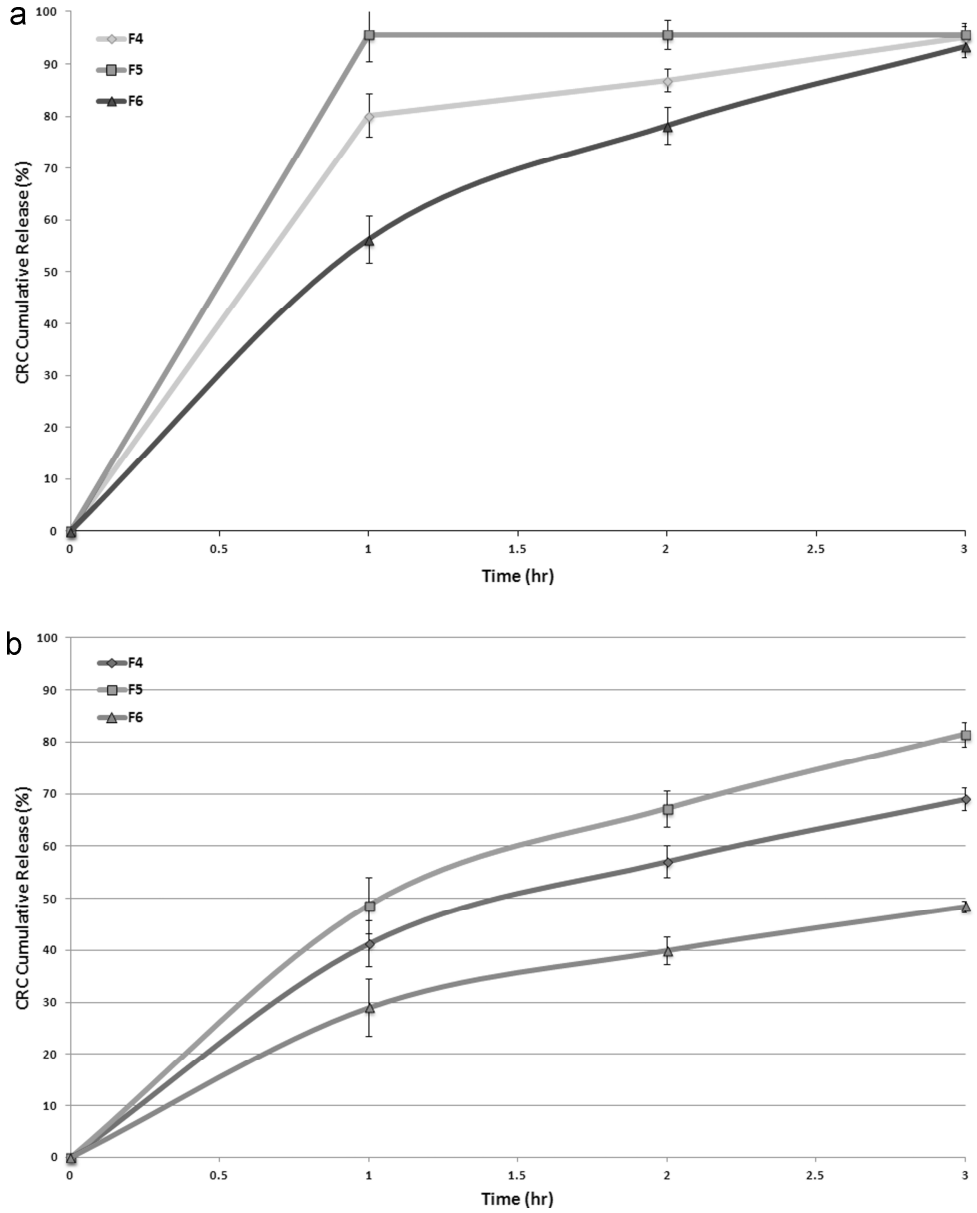

Fig. 6

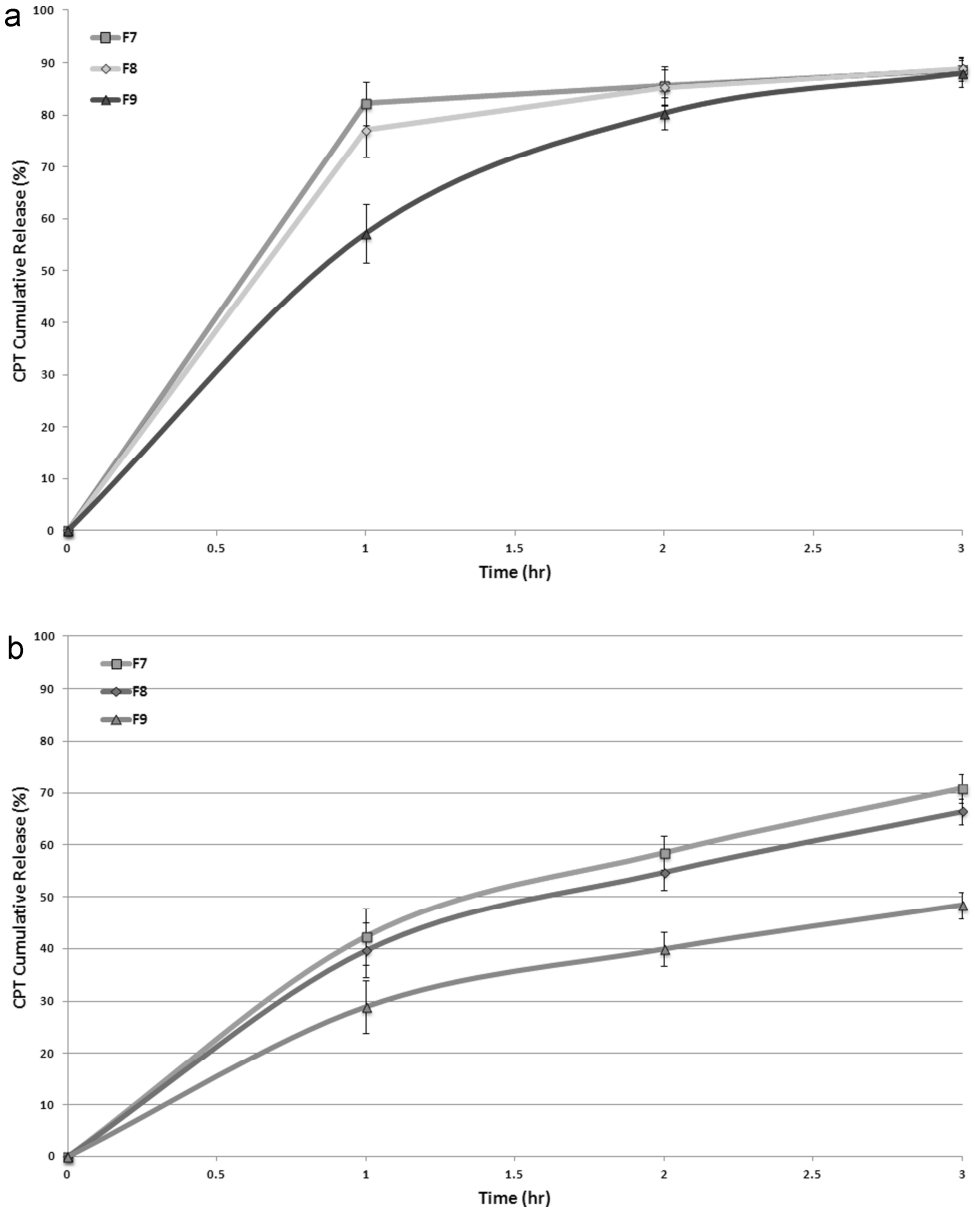

Fig. 7

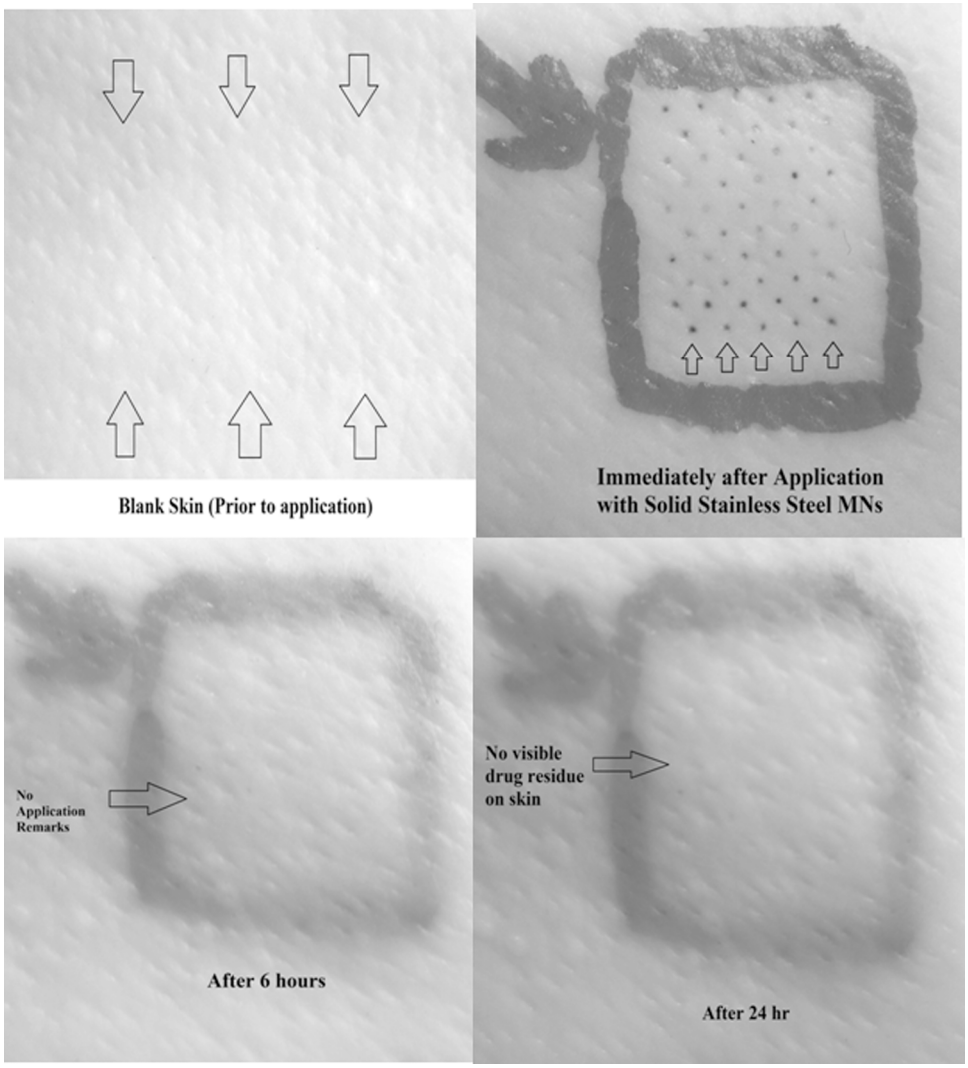

Fig. 8